Structural Evolution and Heterogeneities Studied by Frequency-Dependent Dielectric Sensing in a Styrene/Dimethacrylate Network

Z. Guo,[†] H. Sautereau,[‡] and D. E. Kranbuehl*,[†]

Departments of Chemistry and Applied Science, College of William and Mary, Williamsburg, Virginia 23185-8795, and Laboratoire des Materiaux Macromoleculaires, UMR CNRS 5627, Institut National des Sciences Appliquees, Villeurbanne Cedex 69621, France

Received April 13, 2005; Revised Manuscript Received July 19, 2005

ABSTRACT: Frequency-dependent dielectric sensing and differential scanning calorimetry (DSC) are used to observe the formation of a spatial heterogenety in a dimethacrylate-based network system during polymerization. The presence of two α-relaxation processes as observed in the dielectric sensing measurements very early during the polymerization supports the existence of two cooperative regions of sufficient size to create two T_g's. The two regions do exhibit two T_g's detected by DSC as well as the separately identifiable dielectric α-relaxations. This heterogeneity in the styrene/dimethacrylate system is due to the formation of microgels shortly after reaction initiation. The microgels and their agglomeration form cross-linking regions in a pool of unreacted monomers and oligomers. With the advancement of the reaction, the microgels become larger and start to grow into the monomer−oligomer region. Near the end of the reaction, the low-frequency tail of the microgel and high-frequency portion of the oligomer regions overlap, forming a very broad distribution in the dielectric response and a very broad T_g temperature transition spanning 200 °C in the DSC profile.

1. Introduction

Highly cross-linked polymers made by free radical polymerization of multifunctional monomers have desirable properties for a wide variety of applications.[1−9] A particularly interesting property of these materials is their potential to exhibit spatial heterogeneity due to the formation of microgels,[10−12] domains of high cross-linking density, dispersed in a pool of unreacted monomers. Various experimental techniques have been used by others[13−24] to investigate the structural heterogeneous formation process during network evolution.

Frequency-dependent dielectric sensing (FDEMS) is a particularly insightful method as it monitors the dipolar reorientational motion of molecules in a polymer.[25−29] This paper reports on dielectric relaxation measurements of the molecular mobility and differential scanning calorimetry (DSC) measurements of the buildup in T_g during the polymerization of the dimethacrylate/styrene resin. There are numerous dielectric research publications on epoxy−amine curing systems. This paper is one of only a few dielectric studies made on the polymerization process of a dimethacrylate resin,[30,31] although a number of papers focus on an acrylate polymers[17,32−37] and blends.[38−46]

A particular objective of this paper is to explore the existence of spatial heterogeneity during cure of this system. The hypothesis of a spatial heterogeneity during cure of a network was initially proposed by Dusek et al.[10−12] The existence of a spatial heterogeneity in cured dimethacrylate resins has been characterized by Bowman et al.[13−15] Early experimental results suggesting the existence of a spatial heterogeneity are found in the earlier work by Landin and Macosko,[43] Hamilec et al.,[44−46] and Kloosterboer et al.[47−49] These groups observed that the reactivity of pendant functional groups in the cross-linked regions was much less than free active vinyl groups. While a correct observation, it is not the full explanation for the existence of the spacial heterogeneity they proposed. This was explained as due to the fast polymerization at the radicals resulting in localized network formation and thereby producing poor compatibility with the regions containing monomer/oligomer components in the system by Dusek et al.,[10−12] Pascault et al.,[42] and Kloosterboner et al.[48]

This paper focuses on the evolution of the dipolar dielectric loss $\epsilon_d''(\omega,t,T)$ as the sample cures at different temperatures (T), frequency (ω), and time (t) while achieving different conversions (α). Our interest is to relate the changes in molecular dipolar mobility to the development of the heterogeneity. Another interest is to characterize the glass transition regions in the DSC profiles. Dielectric spectra and the DSC's T_g profiles are used together to characterize the evolution of the heterogenity during the buildup of the styrene/dimethacrylate-based network. Then the dielectric spectra and DSC T_g profiles are used to investigate the existence of two cooperative regions of sufficient size to create two α-relaxation processes representing oligomer-rich and polymer microgel regions during the polymerization.

2. Experimental Section

2.1. Materials. Styrene (St) from Adrich (20 wt %) was mixed with dimethacrylate of tetraethoxylated bisphenol A (D121) from Akzo-Nobel or CD540 from Cray Valley (80 wt %) to form the D121/St mixture. Then 0.5 phr of chain transfer agent 1-dodecanethiol (Aldrich) and 0.2 phr of initiator azobis(methylbutyronitrile) (Aldrich) were added to the mixture. The chain transfer efficiently reduces the kinetics chain length. It has been reported this will decrease the system heterogeneity during the reaction.[50,51] All products were used as received. Table 1 shows the formulas of these two reactants.

The mixing was carried out in a glass vial with a magnetic stirrer and argon bubbling at ambient temperature for 30 min to ensure a homogeneous blend of all components and to

[†] College of William and Mary.
[‡] Institut National des Sciences Appliquees.
* Corresponding author: Tel +1-757-221-2542; fax +1-757-221-2540; e-mail dekran@wm.edu.

10.1021/ma050788b CCC: $30.25
Published on Web 08/18/2005

Table 1. Chemical Products Used in Synthesis of Materials

Name	Chemical formula
Dimethacrylate of tetraethoxylated bisphenol A (D121)	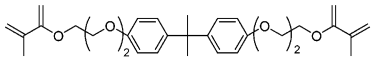
Styrene (St)	
1-Dodecanethiol	$CH_3(CH_2)_{11}SH$
azobis(methyl-butyronitrile)	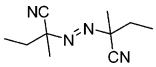

remove oxygen in order to avoid inhibition. Further details of the sample preparation have been previously described in papers by Rey et al.[21,24]

2.2. Dielectric Impedance Measurements. The liquid mixture was introduced into a mold made of two glass plates separated by a 4 mm rubber gasket. A thin sample was needed to maintain a constant temperature during this exothermic reaction. A microsensor from Century Circuit & Electronics consisted of interdigitated copper electrodes (50 μm in width with a spacing of 86 μm) on an area of 2.5 × 1.2 cm flexible polyimide substrate was enclosed in the cell. The electrodes were linked to a HP 4192A impedance analyzer by wires to measure the conductance and capacitance of the materials over a range of temperature and frequency.

The enclosed cell was placed in an oven at a constant temperature for cure. The dielectric permittivity and dielectric loss were measured at eight frequencies in the range from 50 Hz to 250 kHz. The measurement was taken every 2 s across all the frequencies. A computer acquired the dielectric data automatically. The frequency-dependent dielectric data were used to monitor changes in the dielectric properties vs time during cure and then vs temperature for samples at various degrees of conversion. The frequency dependence of the dielectric loss was used to characterize changes in the α-relaxation processes during the polymerization and to investigate the existence of two distinct dynamic regions in the system at certain extents of the cure.

2.3. DSC Measurement. *2.3.1. Kinetics.* A TA 2920 modulated DSC (DSC) was used for the thermokinetic studies. The thermal analysis consisted of an isothermal conventional DSC run to determine reaction heat Q_i at that temperature and then followed by a dynamic ramp to a suitable high temperature to determine the residual heat of polymerization Q_r for all the samples. The conversion at a given time, $\alpha(t)$, was approximately calculated from

$$\alpha(t) = Q_t/(Q_r + Q_i) \tag{1}$$

where Q_t is the heat produced by the reaction at the time t. These heats are a combination of the heats given off by the St−St, St−D121, and D121−D121 reactions and thus represent an approximation of the extent of double bond conversion. However, since in this 80% dimethacrylate and 20% styrene mixture the dimethacrylate and styrene react at the same rate, this approximation is quite accurate. Details of this reaction were reported previously.[21,24]

2.3.2. Glass Transition (T_g) Measurements. During the 70 °C isothermal cure, the reactant in DSC pan was quenched to −100 °C after reacting for a period of time and then heated to 70 °C at 5 °C/min to characterize the glass transition at different conversions using the inflection point as determined by the TA Instruments software.

2.4. Rheology. A TA Instruments AR 1000 rheometer was used to measure the viscosity changes and detect the gelation during the isothermal cure: 40 mm diameter aluminum parallel plates separated with a sample thickness of 2 mm were used in the measurements. Liquid monomer were loaded and housed inside an environmental test chamber. The storage G' and loss G'' modulus were measured at regular intervals, from 0.1 Hz to 1 kHz, at zero normal force. The gel point was determined from the time at which tan δ became independent of frequency.[42]

3. Results and Discussion

3.1. Dielectric Measurements during Isothermal Cure. Dielectric measurements were performed on the free radical copolymerization of D121/St at 60, 70, and 80 °C. Figure 1a−c shows the loss component ϵ'' of the permittivity scaled by the frequency vs time during the isothermal cures. Plots of the product of the dielectric loss (ϵ'') multiplied by the frequency ($\omega = 2\pi f$) make it easy to visually determine the ionic mobility contribution to the dielectric loss which is observed by the overlapping lines at the low frequencies. The absence of low-frequency lines in Figure 1 below the overlapping lines demonstrates the absence of charge polarization effects which create an apparent lower conductivity. The contribution of rotational mobility of bound charge to the dielectric loss is observed by the peaks in the spectrum at high frequencies.

Thus, the dielectric loss generally observed at high frequencies is a combination of the dipolar part (d) and ionic charge part (i).

$$\epsilon'' = \epsilon_d'' + \epsilon_i'' \tag{2}$$

As seen in Figure 1, the low-frequency dielectric loss ϵ'' shows overlapping values up to 200 min at 60 °C in Figure 1a and up to100 min in Figure 1b. These values can be used to determine a frequency-independent conductivity using eq 3:

$$\sigma\,(\Omega^{-1}\,\mathrm{cm}^{-1}) = \epsilon_0 \omega \epsilon_i''(\omega)$$

$$\epsilon_0 = 8.854 \times 10^{-14}\,\mathrm{C}^2\,\mathrm{J}^{-1}\,\mathrm{cm}^{-1} \tag{3}$$

The dielectric loss ϵ'' at high frequencies in Figure 1a−c shows distinct peaks during the isothermal curing. These peaks are due to the dipolar mobility being close at that time and temperature to the frequency or time scale of the oscillating electric field. This dipolar contribution to ϵ'' can be determined more accurately by subtracting the ionic component.

$$\epsilon_d'' = \epsilon'' - \sigma/\epsilon_0\omega \tag{4}$$

The gel time measured by dynamic rheological tests agrees with the results in Rey et al.'s paper.[24] At 70 °C, gelation occurs at a total conversion of 14% after 28 min. The results for all three temperatures are reported in Table 2. Table 2 shows that the molecular gelation has no corresponding event in the ionic mobility as measured by the dielectric loss for this system. This strongly supports the view that fundamentally the dielectric spectrum is not associated with the gelation event. This is because ionic conductivity at low frequencies monitors in general the motions on a much smaller scale than those being affected by macroscopic gelation. Thus, the gelation process should not and clearly in this case is not observed through dielectric spectroscopy as previously suggested in some articles.[52,53]

The peaks in ϵ'' dipolar (which are usually close to the peak in ϵ'') can be used to determine the time or point in the cure process when the "mean" dipolar relaxation time has attained a specific value comparable to the time scale of the frequency of the applied force.

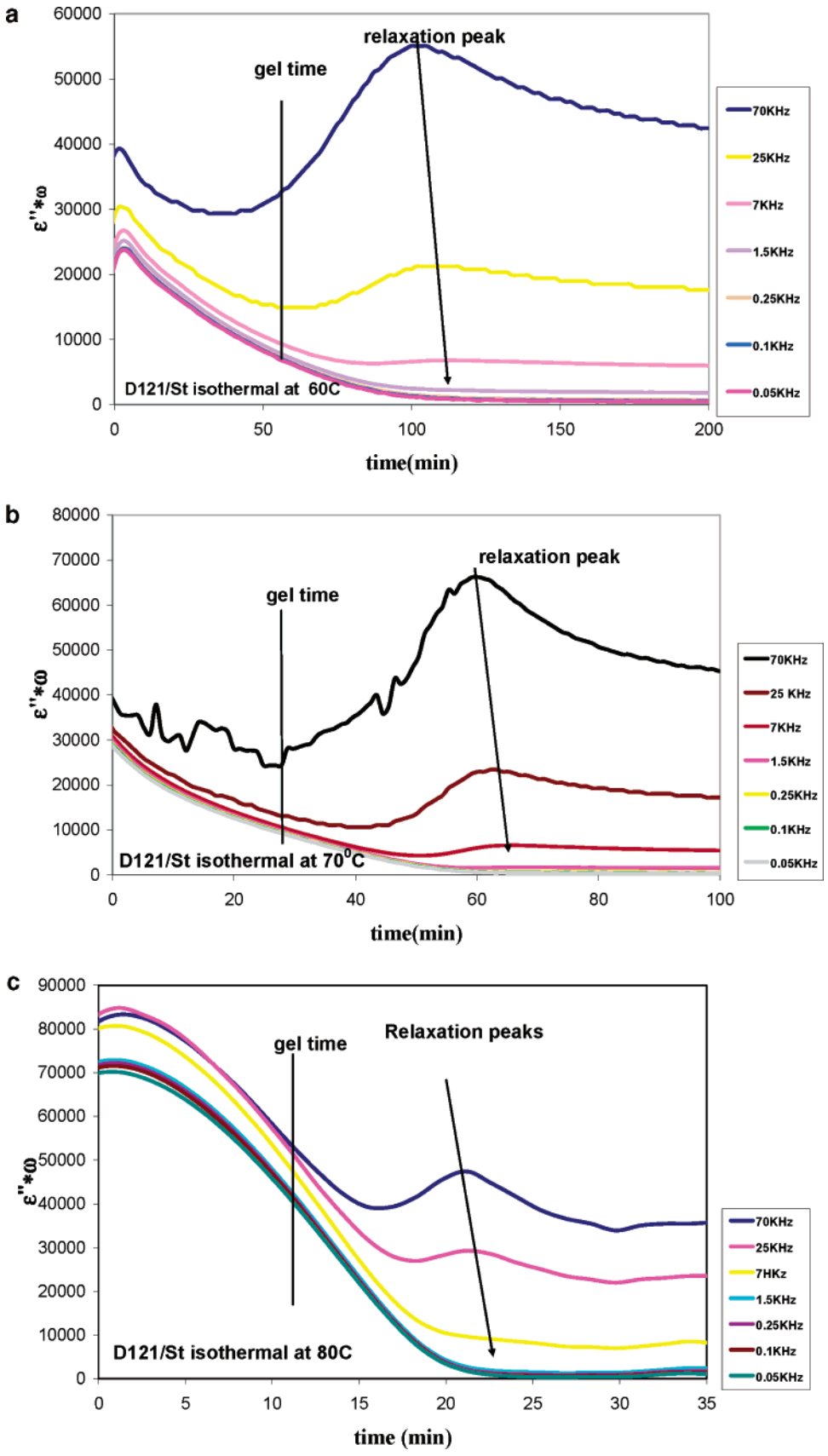

Figure 1. (a, b, and c) $\epsilon''*\omega$ vs time during 60, 70, and 80 °C isothermal polymerization of D121/St. The lowest three frequencies lie on top of each other.

At the time of a peak, a relaxation time characterizing molecular dipolar mobility can be calculated from $\tau = 1/\omega$. These relaxation times monitor the α relaxation process associated with vitrification. The peaks at different frequencies represent the time during conversion at which the materials appear to behave as a glass

Table 2. Gel Times (min) and Inflection Point in the Dielectric Loss Spectra (at 0.1 kHz) during Isothermal Cure for D121/St

temp (°C)	60	70	80
gel time (min)	64	28	13

Table 3. Total Conversion, T_g Temperatures Determined by DSC, and T_g Temperatures Determined by Dielectric Measurement (2.5 kHz) at Different Curing Cycles for D121/St Shown in Figure 2

time (min)	total conv[a] (%)	$T_g(1)$ (°C)	$T_g(2)$ (°C)	$T_{\alpha 1(2.5\ kHz)}$ (°C)	$T_{\alpha 2(2.5\ kHz)}$ (°C)
0	0	−64		−46	
15	5	−62	−41	−45	−18
30	19	−56	−15	−41	−7
50	41	−44	0	−32	6
70	88		10	−34	*b*

[a] Acrylic and styrene monomers. [b] Too broad.

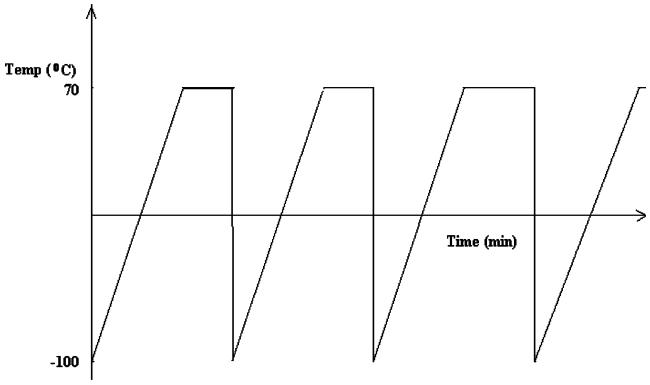

Figure 2. Temperature−time procedure used to determine T_gs at different degrees of cure during 70 °C isothermal polymerization.

at that frequency and corresponding time scale. Thus, these peaks can be used to probe the build up in time of T_g during the isothermal cure.

3.2. Dielectric Relaxation and the DSC Profile during a Temperature Ramp. As seen in Figure 1a−c, the relaxation time of the α relaxation process changes with the increase in the glass transition temperature as the reaction advances, producing a series of $\epsilon''_{dipolar}$ peaks for the D121/St system during the isothermal cure. But even with the modulated DSC, it is hard to determine the calorimetric glass transition during the isothermal cure. This is because the amount of heat created during the polymerization conceals the glass transition's thermal event during cure and particularly because the temperature width of the glass transition is large. Thus, another temperature−time reaction procedure shown in Figure 2 was used to investigate and compare the changes in both the dielectric dynamic and the calorimetric glass transitions during the polymerization.

In this procedure, the unreacted monomer mixture was cooled to −100 °C and heated back to the curing temperature at a constant rate. Then, it was held at the curing temperature for a period of time. After the reactant was partially reacted, it was quenched again to −100 °C and heated back to curing temperature at a constant rate. The quenching and heating steps are repeated several times until the system is cured. Table 3 shows the extent of conversion of the styrene and methacrylate double bonds after each cycle as measured by DSC.

First we examine the information in the cure sequence shown in Figure 2 using dielectric sensing. Figure 3a−e displays the dielectric results for the temperature ramp steps during the cure. Only the α-relaxation peak for the monomers in the unreacted mixture was observed at the beginning of the reaction. As the extent of conversion increases, two distinct relaxation peaks are observed. We believe they are both α-relaxations for the D121/St system. We associate the higher temperature peak with vitrification of the microgel D121/St network. A much faster α-relaxation peak at a lower temperature remains throughout most of the cure reaction. This peak was associated initially by Bowman to the pools of monomer's T_g and then to short oligomeric structures as the reaction advances.[15] We agree and associate this peak with the monomer−oligomer region. Table 3 reports the values of the temperatures of the α-relaxation peaks observed as the reaction progresses at a frequency time scale of 2.5 kHz.

Next we report the results of this cure sequence using DSC. Figure 4 shows the DSC profiles during the temperature ramp for D121/St at different degrees of conversion. The monomer/oligomer glass transition is observed at −64 °C. As the conversion increases, a second T_g transition is observed at a higher temperature in addition to the monomer−oligomer T_g transition for D121/St. The heat capacity change of the first transition is about 0.3 J/(g K), which is close to an expected value of about 0.5 J/(g K). The second transition is much smaller as the fraction of mass in the network state is also small. Table 3 reports values of the T_g's observed in the DSC spectra. The glass transition of the 88% conversion sample is very broad, and the $T_g = 10$ °C for this sample is a calorimetric software determined value, which conflicts with the visual appearance of a glass at room temperature.

For the monomer mixture, the system is homogeneous, and only one relaxation process exists. As the polymerization proceeds, the environment becomes more and more restricted for radical diffusion. As Dusek et al. suggested,[10−12] the radicals trapped in polymer-rich regions produce the growth in the microgel structure. This in turn results in the system becoming heterogeneous and another relaxation response in the dielectric spectra is generated in addition to the monomer−oligomer relaxation response. As seen in Table 3, the results show that the T_g's and the α-relaxation temperatures for the two relaxation peaks reflect the change in T_g in each region. In the dielectric spectra, especially at low conversion, the monomer/oligomer α-relaxation is dominant. The α-relaxation of the microgel polymer network at low conversions is hidden by the tail of the strong monomer/oligomer α-relaxation peak. Thus, the temperatures reported in Table 3 for the microgel α-relaxation peak at the lowest degrees of conversion are approximate.

The dielectric α-relaxation peaks correspond to the temperature at which the time scale of dipolar mobility is comparable to the applied frequency. The increasing cooperativity of the dynamics increases these relaxation times with the extent of reaction. The calorimetric glass transition measured by DSC monitors the chain's segmental motions effect on the heat capacity. Empirically it has been reported that the calorimetric glass transition temperature corresponds to an approximate relaxation rate which corresponds to a much lower frequency of 10^{-3}−10^{-2} Hz.[54]

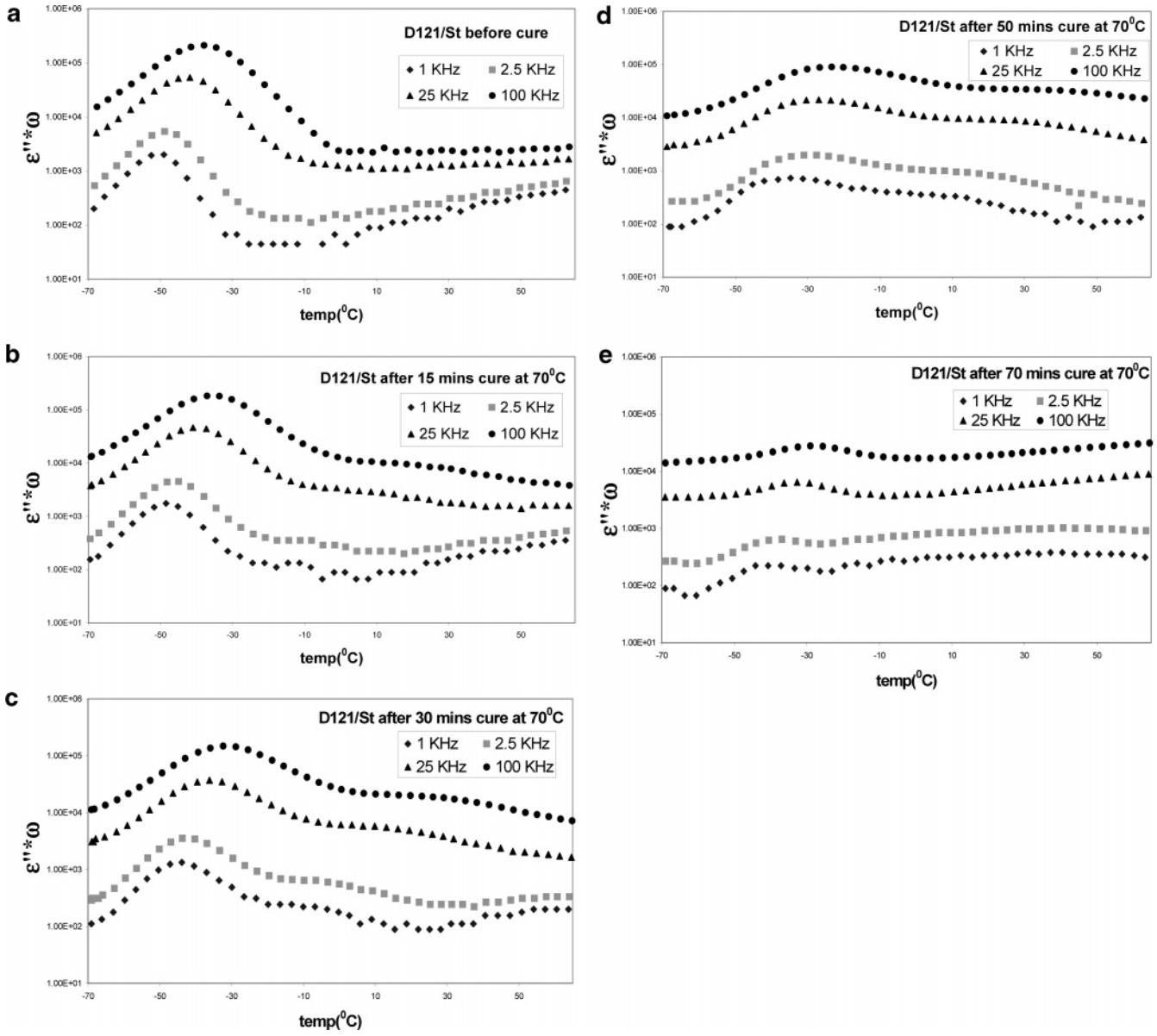

Figure 3. (a−e) $\epsilon''*\omega$ vs temperature at different total conversions.

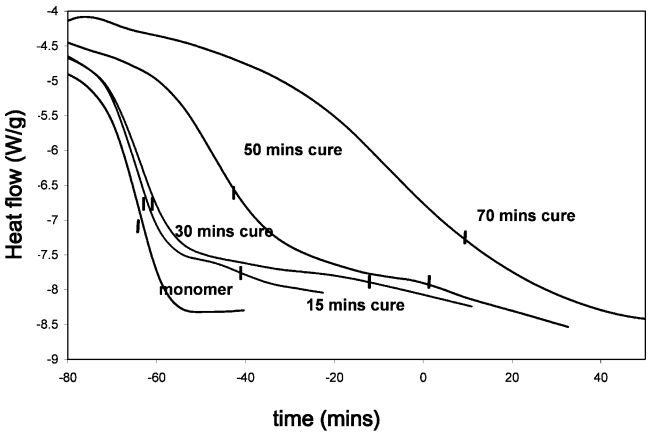

Figure 4. T_g evolution during 70 °C isothermal polymerization of D121/St (the T_g mark (|) is determined by TA Instruments software).

The formation of spatial heterogeneity during the cure for D121/St was also observed in atomic force microscopy (AFM), dynamic light scattering (DLS), and positron annihilation lifetime spectroscopy (PALS) measurements.[21−24] Three distributions of particles, which related to oligomer, single microgel, and microgel clusters, were observed in DLS analysis. Further, a nodular structure was observed in AFM graphs.[24] This nodular structure is a consequence of the network buildup through the formation of microgels and their growth into clusters.

3.3. WLF Equation Fitting for the Relaxation Peaks. The temperature dependence of the relaxation rate of the α-relaxation can be parametrized by the Williams−Landel−Ferry (WLF) equation near the glass transition temperature:[55]

$$\log(\tau/\tau_0) = -C_1(T - T_0)/(C_2 + T - T_0) \qquad (5)$$

where τ is the relaxation time for molecules and T_0 is a reference temperature. C_1 and C_2 are constants related to the fractional free volume (ν_0) and thermal expansion coefficient (α_f) of the free volume at T_0.

The monomer/oligomer relaxation peaks at different frequencies are quite obvious in the dielectric spectra (Figure 3a−e). The relaxation rate τ and corresponding

Table 4. D121/St Monomer/Oligomer WLF Fitting Parameters

conv (%)	T_g (°C)	C_1	C_2 (K)	R^2
0	−64	12.04	19.81	0.996
5	−62	13.19	23.73	0.975
19	−56	13.98	24.41	0.998
41	−44	15.24	26.50	0.919

temperature T at different conversions are determined from the dielectric spectra and fitted with the WLF equation (eq 5), which can be written in the form

$$-(T - T_0)/\log(\tau/\tau_0) = (T - T_0)/C_1 + C_2/C_1 \quad (6)$$

The following procedure is used to determine the constants C_1 and C_2: First, the calorimetric glass transition temperature T_g was chosen as the reference temperature at different conversions. $\tau = 100$ s was chosen due to the relation between the relaxation rate and T_g.[54] Then, $-(T - T_0)/\log(\tau/\tau_0)$ and $T - T_0$ were calculated at different relaxation rates The constants C_1 and C_2 were calculated from the slope and intercept using eq 6. The resulting WLF parameters C_1 and C_2 at different conversions are listed in Table 4.

The WLF fitting results indicate that the WLF parameters C_1 and C_2 are increasing functions of conversion for monomer/oligomer α-relaxation processes. C_1 is inversely proportional to the fractional free volume (ν_0) in the material at the temperature of interest. The increase of C_1 indicates the movement of the molecules becomes restricted with the advancement of the reaction as the free volume decreases. This result is consistent with the free volume study made by Rey et al. for the D121/St system.[23] C_2 equals the fractional free volume (ν_0) divided by the thermal expansion coefficient (α_f). Normally, the thermal expansion coefficient decreases with the cross-linking density of the materials.[56−58] The slight increase of C_2 suggests the thermal expansion coefficient decreases faster than the free volume during the polymerization. The thermal expansion coefficient (α_f), which is inversely related to the product of C_1 and C_2, is observed to decrease with the advancement of the reaction. Another observation for C_1 and C_2 is that the values of C_1 and C_2 approach 17.44 and 51.5, which are the universal values for the WLF equation for a polymer with $T_0 = T_g$. This means that the monomer/oligomer region is shifting toward polymer region values slowly with the advancement of cure.

Accurate fitting of the microgel α relaxation peaks with WLF function is not possible due to the tail of monomer/oligomer peaks.

3.4. Width of the Relaxation Peaks. In general, the relaxation peaks when observed at a fixed temperature move from a high frequency to a low frequency as the reaction advances. The width of the ϵ'' vs frequency (f) plot at half-height, $\Delta\log(f_{1/2})$, increases and the strength of the relaxation peaks decreases with reaction advancement. For the unreacted mixture, the α-relaxation response is narrow because the molecules and domains of cooperative interaction are smaller and of similar size. As the reaction progresses, with the buildup of the microgel network regions, many molecules remain as an oligomer/monomer in other regions. The increasing distribution in the size and regions of the monomer/oligomer molecules in the resin causes a broadening of the relaxation spectrum as be measured by $\Delta\log(f_{1/2})$ in the monomer/oligomer regions.

Table 5. Shape Parameter (β) Determined by Half-Height Width of Relaxation Peak (Δ) of D121/St Monomer−Oligomer Region

time (min)	conv (%)	$\Delta\log(f_{1/2})$	β
0	0	1.96	0.58
15	5	2.79	0.41
30	19	3.34	0.32
50	41		
70	88		
	a		0.11

[a] Fully cured data is measured by dynamic mechanic rheometer (cited from ref 21).

The half-width ($\Delta\log(f_{1/2})$) value is a quantity first proposed by Moynihan et al. which can be used to estimate the parameter (β) of the stretched exponential relaxation decay function $\phi(t)$ for the monomer/oligomer glass transition regions, where[59−62]

$$\phi(t) = \exp(-t/t_0)^{\beta} \quad (7)$$

β indicates the distribution in the dipolar mobilities, or relaxation times, in the system. The β values calculated from half-widths ($\Delta\log(f_{1/2})$) for the monomer−oligomer relaxation spectrum are listed in Table 5. The parameter β varies between 0 and 1. A value close to zero implies a very board distribution of relaxation times, and a value close to 1 implies a narrow distribution of relaxation times. Generally, a polymer's high frequency β-relaxation spectrum displays a broad dielectric loss peak with half-widths of 4−6 decades.[54,63] The half-width ($\Delta\log(f_{1/2})$) values in Table 5 are all less than 4 decades. This is consistent with these low-temperature peaks being associated with the α-relaxation of the monomer−oligomer region.

As seen in Table 5, the value of β for the monomer−oligomer α-relaxation region decreases from 0.58 to 0.32 during the initial 30 min of the polymerization as the conversion increases to 19%. At 50 min and a conversion of 41%, the breadth of the monomer−oligomer α-relaxation overlaps the already broad α-relaxation spectrum of the microgel regions. At this point in the reaction as already discussed, microgel networks are extending into the monomer−oligomer regions. As the reaction progresses beyond this point, the overlap of the α-relaxation processes of these two regions continues to increase. This is observed in Figure 3d,e at 50 and 70 min. At this point, a very broad α-relaxation process is observed which extends over more than 100 °C. Evidence of two relaxation regions remains, as seen by the apparent maxima in the loss around −30 and +30 °C.

The breadth of the combined α-relaxation processes of these two regions has been characterized also by dynamic mechanical measurements of the fully cured resin as reported in Table 5.[21] The value of β as determined from the total width of the dynamic mechanical measurements decreased to 0.11, and the total width of the α-relaxation processes of both regions as characterized by the dynamical mechanical measurements extended from −50 to 200 °C.[21]

Overall, these results are in good agreement with a number of observations and conclusions made by Christopher Bowman based on dielectric and mechanical measurements on cured dimethyl acrylate networks.[13−15] In their studies, they observed two distinct relaxation regions. The higher mobility relaxation spectrum was attributed to "monomer pools" of unreacted double bonds. This relaxation process was separate and in

addition to a "primary" peak at low frequencies. The high-temperature relaxation spectrum was attributed to the glass transition. Taken together, these two peaks implied a "very high degree of structural heterogeneity". They are indeed similar to the spectra observed here as our dimethacrylate system approaches full cure. What is now clear is that the secondary high mobility peak is the dominant peak throughout the initial stages of the reaction and that the microgel, lower mobility peak occurs very early on in the course of the reaction. This low-frequency, high-temperature relaxation is observed here after only 15 min at 5% conversion, before "macroscopic gel", by both our dielectric and differential scanning calorimetry measurements.

3.5. Summary Network, Monomer Heterogeneity. In summary, in the very early stages of the reaction, a polymer microgel region builds up. The increasing molecular connectivity forms polymer domains with different size from the monomer/oligomer domains.[24] Because of the existence of the microgel domain, a new lower frequency, higher temperature α-relaxation process appears in the dielectric spectra. The polymer microgel relaxation peak appears as a shoulder on the monomer/oligomer relaxation peak after only 15 min of cure (Figure 3b). Formation of the microgel region as detected by the dielectric technique is observed much earlier than the gel time (28 min) measured by rheometer. With the advancement of the reaction, these two α-relaxation peaks begin to separate and form two distinct peaks as seen in Figure 3d. During the initial 30 min, Figure 3b−d indicates the dipolar mobility in the polymer clusters decreases rapidly, while the dipolar mobility in the monomer/oligomer region changes less as the conversion increases.

In the early stages of the reaction, the related glass transition buildup in the polymer microgel region can be observed in DSC spectra (Figure 4). At the beginning of the reaction, no microgel region existed in the D121/St system. As reported with the advancement of the reaction at 15 min, $\alpha = 5\%$, two thermal glass transitions are observed in Figure 4. This Figure shows that during the initial 30 min the glass transition of the microgel region shifts from low temperature to high temperature as does the glass transition of monomer/oligomer region. As in the dielectric spectra, the change in T_g in the monomer−oligomer region is at a slower rate than in the microgel region. During the later stages of the reaction, the monomer−oligomer glass transition, as observed by DSC, extends into the microgel glass transition due to the now interconnected network between microgels and oligomers in the resin. During the later step, peaks of the microgel region shows the same overall behavior as α-relaxation time. The peaks shift to a higher temperature, and the distribution becomes wider as the conversion increases. This produces one very board glass transition event and a very broad α-relaxation spectrum at 70 min, 88% conversion as is observed in the DSC spectra.

4. Conclusion

The heterogeneous formation of a monomer/oligomer region and a microgel region was characterized with in situ dielectric and DSC measurements during the polymerization reaction.

In the D121/St system, two distinct T_g, α relaxation responses are observed very early and prior to macroscopic gel during polymerization in both the dielectric and DSC spectra. They correspond to two spatially distinct regions: a glass transition in monomer/oligomer regions and a glass transition in the polymer microgel regions.

For each region, with the advancement of the reaction, the distribution of the relaxation times and the temperature breadth of both glass transitions increase. As the reaction advances toward completion, these two regions and their spectrum broaden and extend into each other to create a very broad relaxation spectrum, reflecting a spatial heterogeneous continuum characterized by a very small β and a T_g temperature transition spanning 200 °C.

References and Notes

(1) Alloin, F.; Sanchez, J. Y.; Armand, M. *J. Electrochem. Soc.* **1994**, *141*, 1915−1920.
(2) Anseth, K. S.; Newman, S. M.; Bowman, C. N. *Adv. Polym. Sci.* **1995**, *122*, 177−217.
(3) Koo, J.-S.; Smith, P. G. R.; Williams, R. B.; Grossel, M. C.; Whitcombe, M. J. *Chem. Mater.* **2002**, *14*, 5030−5036.
(4) Leung, S. H. S.; Robinson, J. R. *J. Controlled Release* **1988**, *5*, 223−231.
(5) Shah, J.; Ryntz, R. A.; Gunn, V. E.; Xiao, H. X.; Frisch, K. C.; Feldpausch, A.; Kordomenos, P. I. *J. Coat. Technol.* **1989**, *61*, 61−69.
(6) Stansbury, J. W. *J. Dent. Res.* **1992**, *71*, 1408−1412.
(7) Yukawa, Y.; Yabuta, M.; Tominaga, A. *Prog. Org. Coat.* **1994**, *24*, 359−379.
(8) Roice, M.; Kumar, K. S.; Pillai, V. N. R. *Macromolecules* **1999**, *32*, 8807−8815.
(9) Dullens, R. P. A.; Claesson, E. M.; Kegel, W. K. *Langmuir* **2004**, *20*, 658−664.
(10) Dusek, K. *Polym. Gels Networks* **1996**, *4*, 383−404.
(11) Dusek, K. *Angew. Makromol. Chem.* **1996**, *240*, 1−15.
(12) Dusek, K.; Matejka, L.; Spacek, P.; Winter, H. *Polymer* **1996**, *37*, 2233−2242.
(13) Kannurpatti, A. R.; Anderson, K. J.; Anseth, J. W.; Bowman, C. N. *J. Polym. Sci., Part B: Polym. Phys.* **1997**, *35*, 2297−2307.
(14) Kannurpatti, A. R.; Anseth, J. W.; Bowman, C. N. *Polymer* **1998**, *39*, 2507−2513.
(15) Kannurpatti, A. R.; Bowman, C. N. *Macromolecules* **1998**, *31*, 3311−3316.
(16) Simon, G. P.; Allen, P. E. M.; Bennett, D. J.; Williams, D. R. G.; Williams, E. H. *Macromolecules* **1989**, *22*, 3555−3561.
(17) Simon, G. P.; Allen, P. E. M.; Williams, D. R. G. *Polymer* **1991**, *32*, 2577−2587.
(18) Wilson, T. W. *J. Appl. Polym. Sci.* **1990**, *40*, 1195−1208.
(19) Allen, P. E. M.; Simon, G. P.; Williams, D. R. G.; Williams, E. H. *Macromolecules* **1989**, *22*, 809−816.
(20) Anseth, K. S.; Wang, C. M.; Bowman, C. N. *Macromolecules* **1994**, *27*, 650−655.
(21) Rey, L.; Duchet, J.; Galy, J.; Sautereau, H.; Vouagner, D.; Carrion, L. *Polymer* **2002**, *43*, 4375−4384.
(22) Rey, L.; Galy, J.; Sautereau, H.; Lachenal, G.; Henry, D.; Vial, J. *Appl. Spectrosc.* **2000**, *54*, 39−43.
(23) Rey, L.; Galy, J.; Sautereau, H.; Simon, G. P.; Cook, W. D. *Polym. Int.* **2004**, *53*, 557−568.
(24) Rey, L.; Galy, J.; Sautereau, H. *Macromolecules* **2000**, *33*, 6780−6786.
(25) Bonnet, A.; Pascault, J. P.; Sautereau, H.; Rogozinski, J.; Kranbuehl, D. *Macromolecules* **2000**, *33*, 3833−3843.
(26) Baillif, P.; Tabellout, M.; Emery, J. R. *Polymer* **2000**, *41*, 5305−5314.
(27) Boyd, R. H.; Devereaux, R. W.; Thayer, R. B. *Polym. Prepr. (Am. Chem. Soc., Div. Polym. Chem.)* **1990**, *31*, 279−280.
(28) Se, K.; Takayanagi, O.; Adachi, K. *Macromolecules* **1997**, *30*, 4877−4881.
(29) Ngai, K. L.; Mashimo, S.; Fytas, G. *Macromolecules* **1988**, *21*, 3030−3038.
(30) Fournier, J.; Williams, G.; Holmes, P. A. *Macromolecules* **1997**, *30*, 2042−2051.
(31) Espadero Berzosa, A.; Gomez Ribelles, J. L.; Kripotou, S.; Pissis, P. *Macromolecules* **2004**, *37*, 6472−6479.
(32) Dudognon, E.; Bernes, A.; Lacabanne, C. *Macromolecules* **2001**, *34*, 3988−3992.
(33) Dudognon, E.; Bernes, A.; Lacabanne, C. *Macromolecules* **2002**, *35*, 5927−5931.

(34) Schroeter, K.; Unger, R.; Reissig, S.; Garwe, F.; Kahle, S.; Beiner, M.; Donth, E. *Macromolecules* **1998**, *31*, 8966−8972.
(35) Theobald, S.; Pechhold, W.; Stoll, B. *Polymer* **2000**, *42*, 289−295.
(36) Bedekar, B. A.; Tsuji, Y.; Ide, N.; Kita, Y.; Fukuda, T.; Miyamoto, T. *Polymer* **1995**, *36*, 4735−4740.
(37) Calleja, R. D.; Garcia-Bernabe, A.; Sanchez-Martinez, E.; Hormazabal, A.; Gargallo, L.; Gonzalez-Nilo, F.; Radic, D. *Macromolecules* **2001**, *34*, 6312−6317.
(38) Mijovic, J.; Sy, J.-W.; Kwei, T. K. *Macromolecules* **1997**, *30*, 3042−3050.
(39) Sy, J. W.; Mijovic, J. *Macromolecules* **2000**, *33*, 933−946.
(40) Zhang, S.; Jin, X.; Painter, P. C.; Runt, J. *Macromolecules* **2002**, *35*, 3636−3646.
(41) Aihara, T.; Saito, H.; Inoue, T.; Wolff, H.-P.; Stuhn, B. *Polymer* **1997**, *39*, 129−134.
(42) Pascault, J. P.; Sautereau, H.; Verdu, J.; Williams, R. J. J. *Thermosetting Polymers*; Marcel Dekker: New York, 2002.
(43) Landin, D. T.; Macosko, C. W. *Macromolecules* **1988**, *21*, 846.
(44) Zhu, S.; Tian, Y.; Hamielec, A. E.; Eaton, D. R. *Macromolecules* **1990**, *23*, 1144.
(45) Zhu, S.; Tian, Y.; Hamielec, A. E.; Eaton, D. R. *Polymer* **1990**, *31*, 154.
(46) Zhu, S.; Tian, Y.; Hamielec, A. E.; Eaton, D. R. *Polymer* **1990**, *31*, 1726.
(47) Kloosterboer, J. G.; Lijten, G. F. C. M.; Greidanus, F. J. A. M. *Polym. Commun.* **1986**, *27*, 268−271.
(48) Kloosterboer, J. G.; van de Hei, G. M. M.; Boots, H. M. J. *Polym. Commun.* **1984**, *25*, 354−357.
(49) Kloosterboer, J. G.; van de Hei, G. M. M.; Gossink, R. G.; Dortant, G. C. M. *Polym. Commun.* **1984**, *25*, 322−325.
(50) Boots, H. M. J.; Kloosterboer, J. G.; Van de Hei, G. M. M.; Pandey, R. B. *Br. Polym. J.* **1985**, *17*, 219−223.
(51) Boots, H. M. J.; Kloosterboer, J. G. *Ned. Tijdschr. Natuurkde., A* **1984**, *A50*, 45−47.
(52) Parthun, M. G.; Johari, G. P. *Macromolecules* **1992**, *25*, 3254−3265.
(53) Parthun, M. G.; Johari, G. P. *Macromolecules* **1993**, *26*, 2392−2393.
(54) Schonhals, A. In *Dielectric Spectroscopy of Polymeric Materials*; Runt, J. P., Fitzgerald, J. J., Eds.; American Chemical Society: Washington, DC, 1997; pp 81−106.
(55) Ferry, J. D. *Viscoelastic Properties of Polymers*, 3rd ed.; John Wiley & Sons: New York, 1980.
(56) Wang, B.; Wang, Z. F.; Zhang, M.; Liu, W. H.; Wang, S. J. *Macromolecules* **2002**, *35*, 3993−3996.
(57) Meijerink, J. I.; Eguchi, S.; Ogata, M.; Ishii, T.; Amagi, S.; Numata, S.; Sashima, H. *Polymer* **1994**, *35*, 179−186.
(58) Salgueiro, W.; Marzocca, A.; Somoza, A.; Consolati, G.; Cerveny, S.; Quasso, F.; Goyanes, S. *Polymer* **2004**, *45*, 6037−6044.
(59) Moynihan, C. T.; Boesch, L. P.; Laberge, N. L. *Phys. Chem. Glasses* **1973**, *14*, 122−125.
(60) Bartolomeo, P.; Chailan, J. F.; Vernet, J. L. *Polymer* **2001**, *42*, 4385−4392.
(61) Williams, G. In *Dielectric Spectroscopy of Polymeric Materials*; American Chemical Society: Washington, DC, 1997; pp 3−66.
(62) Williams, G.; Watts, D. C. *Trans. Faraday Soc.* **1970**, *66*, 80.
(63) A. Schonhals, F. K. In *Broadband Dielectric Spectroscopy*; Friederich Kremer, A. S., Ed.; Springer-Verlag: Berlin, 2002; pp 349−384.

MA050788B